FIRST INTERIM TOPICAL REPORT

on

A STUDY OF THE MECHANICS OF CLOSED-DIE FORGING

THE USE OF MODEL MATERIALS IN PREDICTING FORMING LOADS IN METALWORKING

to

ARMY MATERIAL AND MECHANICS RESEARCH CENTER

December 30, 1968

by

T. Altan, H. J. Henning, and A. M. Sabroff

Contract DAAG46-68-C-0111

BATTELLE MEMORIAL INSTITUTE
Columbus Laboratories
505 King Avenue
Columbus, Ohio 43201

FOREWORD

This topical report on "The Use of Model Materials in Predicting Forming Loads in Metalworking" covers the review work performed under Contract No. DAAG46-68-C-0111 with Battelle Memorial Institute of Columbus, Ohio, from August 1, 1968, to January 1, 1969.

This work was administered under the technical direction of Mr. Robert Colton of the Army Materials and Mechanics Research Center, Watertown, Massachusetts 02172.

The program was carried out under the supervision of Mr. A. M. Sabroff, Chief of the Metalworking Division, and Mr. H. J. Henning, Associate Chief of the Metalworking Division. Dr. T. Altan, Sr. Scientist, is the current principal investigator.

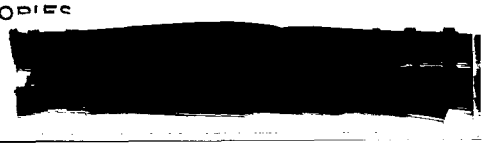

TABLE OF CONTENTS

THE USE OF MODEL MATERIALS IN PREDICTING FORMING LOADS IN METALWORKING

by

T. Altan, H. J. Henning, and A. M. Sabroff

ABSTRACT

The laws of perfect and approximate similarities in metal forming indicate that perfect similarity in deforming two different materials is practically impossible to achieve. Approximate similarity, however, is easy to obtain, and proves to be very useful in predicting forming loads in extrusion and forging processes. Analysis of friction in model experiments shows how interface friction can be taken into account in model studies. Backward and forward extrusion loads are predicted from plasticine model experiments and the results are compared with data for various steels. The agreement between predicted and actual loads is generally well within engineering accuracy. Future work will consist in applying modeling techniques to the non-steady-state process of forging.

INTRODUCTION

Present knowledge of the relationships between material properties, friction conditions, and process mechanics makes an exact theoretical analysis of practical forming operations most difficult. The design of a forming process and the predictions of material flow and of forming loads are largely dependent upon the experience, know-how and intuition of the forming expert. The design of a new forming operation may involve costly trial-and-error experimentation. Thus, a powerful tool in forming research and development is the use of highly deformable model materials to simulate real forming operations. This approach lowers tooling and equipment costs, provides an improved and inexpensive means for proving out tooling modifications, and helps in understanding the specific process being modeled.

Model materials such as wax, plasticine, lead, and clay compositions have been used successfully for obtaining qualitative information about metal flow.[1, 2, 3, 4]* The Visioplasticity method developed by Thomsen and his co-workers[5] can be applied to a model material to obtain quantitative data on material flow, viz., velocity, strain rate, and strain distributions, in various forming operations. The Visioplasticity method, however, involves laborious computations, which have limited its application to basic and fundamental studies. Recently, attempts were made to predict loads and energies in a real forming operation by measuring these variables in a model test and by correlating the properties of the real and model materials.[6, 7, 8] So far, only strain-rate-dependent materials have been considered and the influence of the interface friction has been largely neglected. In the present study, the friction has been considered and forming loads in backward and forward extrusion of various steels have been estimated from model experiments with plasticine.

*References are listed on page 28.

BACKGROUND

Laws of Similarity in Forming

The solution of a forming problem with the mathematical plasticity theory involves solving a system of ten partial differential equations with appropriate boundary conditions. The system of equations involves three equilibrium equations, the von Mises yield condition, and the six Levy-Mises stress-strain rate relations.

Using plasticity theory and introducing the scale factors of length (λ)*, force (κ), and time (T), Pawelski and Kobayashi derived the conditions for elastic, plastic, dynamic, thermal, and gravitational similarity.[9, 10]

The scale factors λ, κ, and T are defined by the following equations:

$$x_R = \lambda\, x_M \tag{1}$$

$$P_R = \kappa\, P_M \tag{2}$$

$$t_R = T\, t_M \quad , \tag{3}$$

where the subscripts R and M designate real and model experiments, respectively, and x denotes length, P denotes force, and t denotes time.

Thus, the similarity conditions with respect to the workpiece are[9, 10]

(a) For plastic deformation

$$\bar{\sigma}_R/\bar{\sigma}_M = \kappa/\lambda^2 \quad , \tag{4}$$

where $\bar{\sigma}$ = flow stress.

(b) For elastic deformation

$$G_R/G_M = E_R/E_M = \kappa/\lambda^2 \quad , \tag{5}$$

where G = shear modulus
E = Young's modulus.

(c) For dynamic forces at high rates of deformation

$$\kappa/\lambda^4 = \frac{\rho_R}{\rho_M} \cdot T \quad , \tag{6}$$

where ρ = specific gravity.

*The symbols are listed in a fold-out page at the end of this report.

(d) For friction forces at interface:

If the friction shear stress is given by Coulomb's law,

$$\mu_M = \mu_R \quad . \tag{7}$$

If the interface shear stress is equal to the shear stress of the workpiece material,

$$\bar{\sigma}_R/\bar{\sigma}_M = \kappa/\lambda^2 \quad . \tag{8}$$

In addition to the above relations, thermal similarity conditions for conduction, convection, radiation heat transfer, and heat generation must be considered for establishing perfect similarity.

Approximate Similarity

Pawelski analyzed in detail the conditions for similarity in the deforming material, the tools, and the forming machine used and concluded that perfect similarity, for all practical purposes, is impossible to achieve in complex problems of metal forming.[9] In particular, satisfying the conditions of thermal similarity is extremely difficult because of material constants involved in heat generation and conduction during deformation. Since for most engineering problems approximate solutions would be sufficient, the methods of approximate similarity must be studied to obtain reasonable correlations between real and model tests.

If the thermal and inertial similarities are not considered, the most important conditions are given by Equations (4) and (7). The condition given by Equation (7), $\mu_M = \mu_R$, explains the experimental observation (widely reported in the literature) that the flow pattern for a given tool geometry will be similar for different materials if

(a) The friction conditions are essentially the same.

(b) The deforming material remains homogeneous during deformation (or the inhomogeneities during deformation remain similar).

The condition expressed by Equation (4) corresponds to the consideration that the flow stress is a function of strain, $\bar{\epsilon}$, strain rate, $\dot{\bar{\epsilon}}$, and temperature, θ, since in any practical forming operation (except homogeneous tensile or compression tests) these variables vary within the deforming material with time. Therefore the deforming material is not, in a strict sense, homogeneous at all and the similarity of the inhomogeneity for two different materials can be obtained only if the functional dependencies of the flow stress, $\bar{\sigma} = \bar{\sigma}\,(\bar{\epsilon}, \dot{\bar{\epsilon}}, \theta)$, are similar. This is actually implied in the perfect similarity condition expressed by Equation (4), which is practically impossible to fulfill.

As pointed out by Brill, a reasonably accurate approximation can be achieved with some materials, at least within a certain range of some variables.[7] For many materials within a certain temperature range, the flow stress is given as an exponential

function of strain, $\bar{\epsilon}$, or strain rate, $\dot{\bar{\epsilon}}$. Thus, in cold forming, $\bar{\sigma} = K\bar{\epsilon}^n$ (K = constant, n = strain-hardening coefficient); in hot forming over the recrystallization temperature, $\bar{\sigma} = C\dot{\bar{\epsilon}}^m$ (C = constant, m = strain-rate-hardening coefficient).

The model experiment can be designed such that the temperature does not vary significantly during deformation. In this case only the dependency on strain rate, $\dot{\bar{\epsilon}}$, or on strain, $\bar{\epsilon}$, must be satisfied in making usefully accurate approximations.

Prediction of Forming Load in a Closed-Die Forging

In his dissertation, Brill studied the flow stresses of different materials at different temperatures and strain rates.[7] As seen in Figure 1, the following relations hold for the effective strain $\bar{\epsilon} = 0.4$:

Paraffin wax at θ = 31 C (88 F), $\bar{\sigma}$ (kp/mm^2)* = 0.044 $(\dot{\bar{\epsilon}})^{0.3}$ (9)

Sodium at θ = 20 C (68 F), $\bar{\sigma}$ (kp/mm^2) = 0.094 $(\dot{\bar{\epsilon}})^{0.22}$ (10)

Steel C45 (AISI 1043) at θ = 1100 C (2012 F), $\bar{\sigma}$ (kp/mm^2) = 7.6 $(\dot{\bar{\epsilon}})^{0.21}$. (11)

The flow stresses, $\bar{\sigma}$, of the above materials do not vary with strain at the given temperatures. Sodium and steel exhibit the same strain-rate-hardening coefficient; i.e., $m_{steel} = m_{sodium}$ in the expression

$$\bar{\sigma} = C\dot{\bar{\epsilon}}^m \quad .$$

Thus, it is expected that sodium at 20 C would simulate the deformation of steel at 1100 C as long as (a) the temperature influences are negligible and (b) distributions of strain rate, $\dot{\bar{\epsilon}}$ (i.e., the flows or the velocity fields) are similar for both materials.

These conditions were satisfied in Brill's experiments, in which a closed-die forging, Figure 2, was used for estimating the forming load in forging steel from the model test with sodium. In order to obtain similar friction conditions, i.e., to satisfy Equation (7), no lubricant was used in forging sodium. The load-displacement curve in Figure 3 shows the excellent agreement between the predicted and the real load-displacement curves.

Generalization of Approximate Similarity

A review of Brill's work shows that it is a difficult task to obtain a model material with flow-stress behavior identical to any given real material, i.e., with equal strain-rate-hardening coefficients (the exponent m in the equation $\bar{\sigma} = C\dot{\bar{\epsilon}}^m$). For most forming operations, however, the flow of the real material can be reasonably well simulated by a model material using similar tool geometry (equal angles, proportional dimensions) and similar friction conditions. Thus, the kinematics of the specific forming operation can be determined in terms of average strain, $\bar{\epsilon}_a$, or average strain rate, $\dot{\bar{\epsilon}}_a$, from the model test. The real forming load can then be estimated from $\bar{\epsilon}_a$ or $\dot{\bar{\epsilon}}_a$ by using the dependency of the flow stress upon $\bar{\epsilon}_a$ or $\dot{\bar{\epsilon}}_a$.

*kp (kilopond) is the new international metric system notation, which replaces kg (kp/mm^2 = 1422.3 psi).

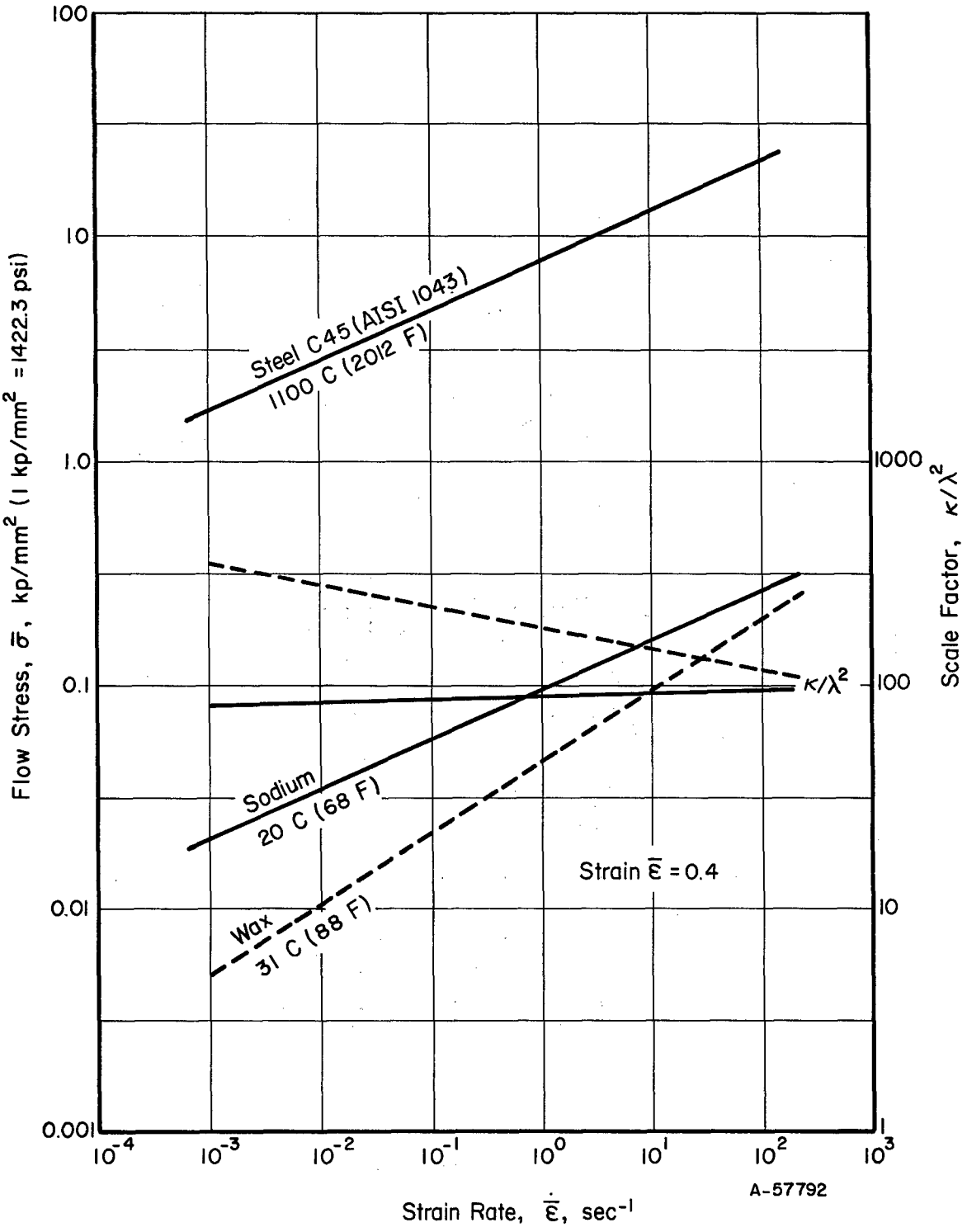

FIGURE 1. DEPENDENCY OF FLOW STRESSES $\bar{\sigma}$ AND SCALE FACTORS k/λ^2 UPON STRAIN RATE $\dot{\bar{\varepsilon}}$ FOR MODEL MATERIALS[7]

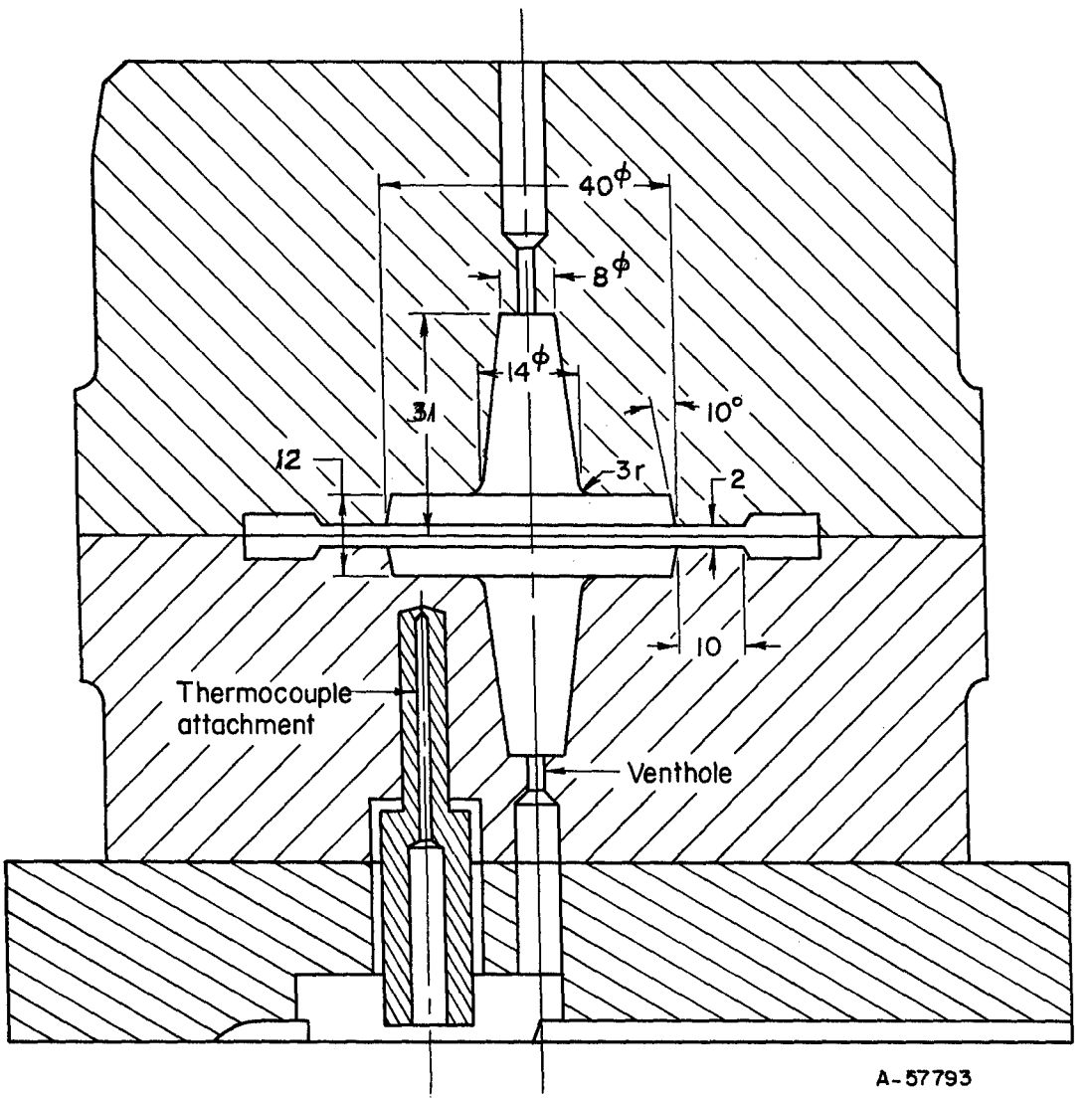

FIGURE 2. AXISYMMETRIC FORGING DIE WITH FLASHGUTTER[7]

Dimensions are in mm, 1 inch = 25.4 mm

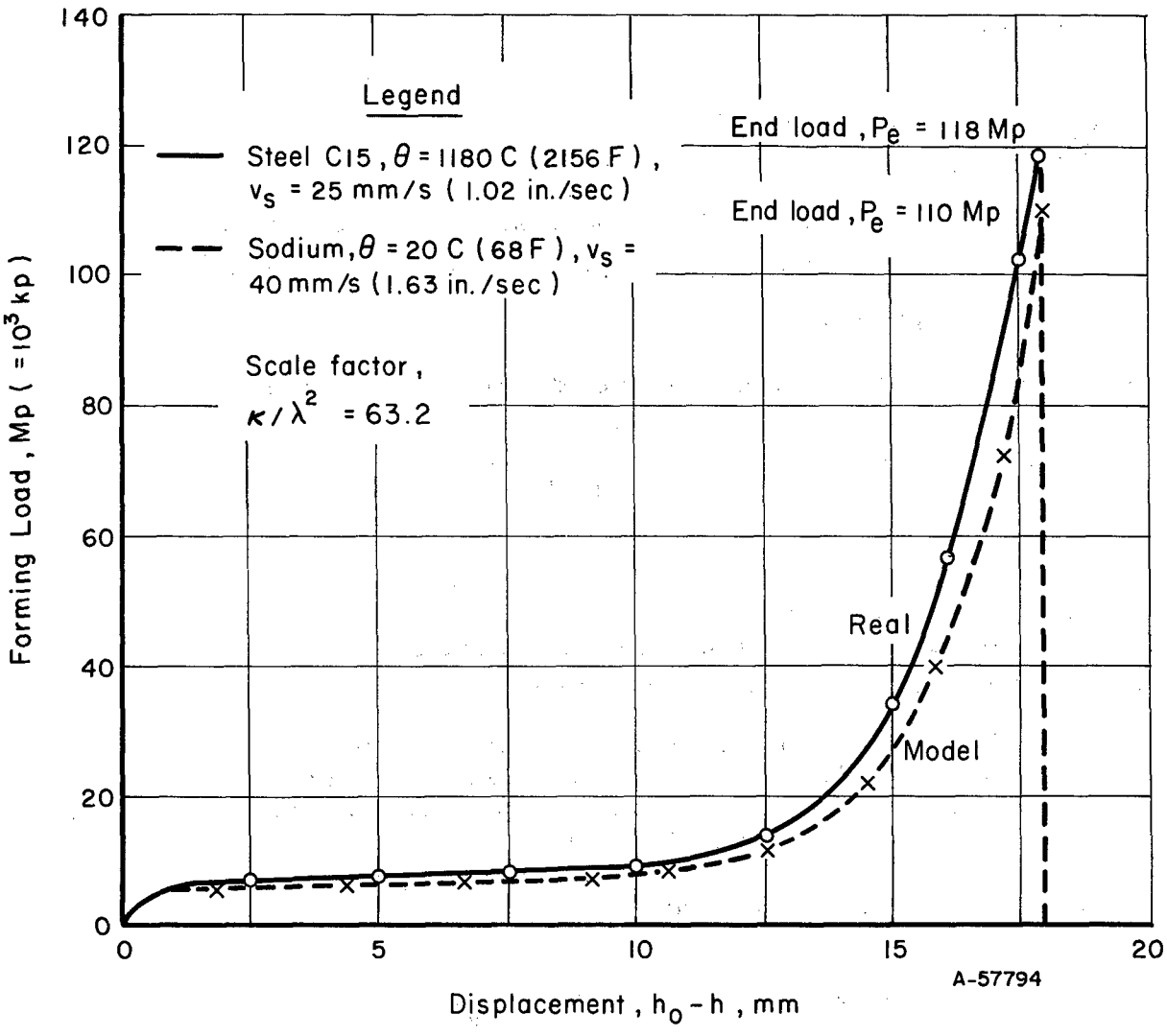

FIGURE 3. FORMING LOAD IN HOT, CLOSED-DIE FORGING OF STEEL C15 (AISI 1043)[7]

Comparison of Real and Model Tests
Samples Forged in Dies Shown in Figure 2

The following conditions can be assumed to hold approximately:

(a) Entropy remains constant during deformation, i.e., no energy in the form of heat is added or subtracted from the deforming body. In hot forming, this would mean that the heat loss to the tools is approximately balanced by the heat generated by deformation and friction.

(b) Both model and real material are homogeneous or exhibit the same inhomogeneity during deformation, i.e., the material flows are kinematically similar.

Approximate Similarity in Strain-Rate-Dependent Materials

The model and the real material are both assumed to be strain-rate dependent according to $\bar{\sigma}_M = C_M \dot{\bar{\epsilon}}^{m_M}$ and $\bar{\sigma}_R = C_R \dot{\bar{\epsilon}}^{m_R}$ (the subscripts M and R represent model and real material, respectively).

The internal and external energy balance during deformation in a time element, (dt), is given by

$$E_o = E_d + E_f \quad , \tag{12}$$

where

E_o = outside input energy per unit time
E_d = internal plastic deformation energy per unit time
E_f = interface friction energy per unit time.

In non-steady-state deformation processes, characteristic of most forging operations, these energies, E_o, E_d, and E_f, vary continuously during deformation. In steady-state operations, where the velocity or the flow field does not vary, significant changes in E_o, E_d, and E_f do not normally occur.

Equation (12) can also be written as

$$p_a \cdot A \cdot v_D \cdot dt = \int_V \bar{\sigma} d\bar{\epsilon} dV + \int_F \tau_F v_F dF dt \quad , \tag{13}$$

where, in addition to the symbols listed at the end of this report,

p_a = average forming pressure

A = cross section upon which p_a is exerted

v_D = die velocity

h = instantaneous average height of deforming material

$V = A \cdot h$ = volume of deforming material

F = interface surface area, contact surface between tool and material

v_F = relative velocity at interface between tool and material

$\tau = f \cdot \bar{\sigma}$ = friction shear stress

f = friction factor, $0 \leq f \leq \frac{1}{\sqrt{3}}$.

The friction shear stress is expressed as a constant value dependent on the flow stress, $\bar{\sigma}$. This is the same convention used in the upper-bound method of analysis and it gives a good approximation, especially at high levels of friction.

Equation (13) illustrates that the external mechanical forming energy introduced by the displacement of the tools during the time dt (left side of Equation 13) is consumed as plastic-deformation energy (first expression on right side of Equation 13) and as friction energy at the tool-material interface (second expression on right side of Equation 13).

With the introduction of strain rate $\dot{\bar{\epsilon}} = \frac{d\bar{\epsilon}}{dt}$, the plastic-deformation energy can be expressed as

$$E_d = \int_V \bar{\sigma} d\bar{\epsilon} dV = \int_V \bar{\sigma} \cdot \dot{\bar{\epsilon}} dV dt = \bar{\sigma}_a \cdot \dot{\bar{\epsilon}}_a \cdot A \cdot h \cdot dt \quad , \tag{14}$$

where

$\bar{\sigma}_a$ = average flow stress over deforming volume $A \cdot h$

$\dot{\bar{\epsilon}}_a$ = average strain rate over deforming volume $A \cdot h$.

The friction energy/unit time can be determined as average values at different zones of the interface by using the friction shear stress, $\tau = f\bar{\sigma}$, with the following derivation:

$$E_f = \int_F f\bar{\sigma} v_F dF = \int_{F_1} f_1 \bar{\sigma}_1 v_1 dF + \int_{F_2} f_2 \bar{\sigma}_2 v_2 dF + \ldots \quad . \tag{15a}$$

where

v_i = relative velocity at interface between tool and material in zone "i" .

Each integral on the right side of Equation (15a) expresses the friction energy/unit time at the interface for a zone of the deforming material. The subscripts 1, 2, etc., designate these different zones of deformation. It is reasonable to assume that, at the interface of a given zone of deformation "i", the flow stress and friction factor f_i would be constant. Thus, Equation (15a) transforms into

$$E_f = f_1\bar{\sigma}_1 \int_{F_1} v_1 dF + f_2\bar{\sigma}_2 \int_{F_2} v_2 dF + \ldots \quad . \tag{15b}$$

Or, using the short summation notation,

$$E_f = \sum f_i\bar{\sigma}_i \int_{F_i} v_i dF = \sum f_i\bar{\sigma}_i I_i \tag{15c}$$

with

$$I_i = \int_{F_i} v_i dF \quad . \tag{15d}$$

Thus, using Equations (14) and (15c), Equation (13) is transformed into

$$p_a A v_D = \bar{\sigma}_a \dot{\bar{\epsilon}}_a A h + \Sigma\ f_i\bar{\sigma}_i I_i \quad . \tag{16}$$

Or, after dividing by $A \cdot h = V$, volume of deforming material

$$p_a v_D/h = \bar{\sigma}_a \dot{\bar{\epsilon}}_a + (\Sigma\ f_i\bar{\sigma}_i I_i)/V \quad . \tag{17}$$

In many cases the following assumptions would hold:

(a) The average flow stress, $\bar{\sigma}_a$, is equal to the flow stress at the interfaces, $\bar{\sigma}_a = \bar{\sigma}_i$; i.e., cooling effects in hot forming are negligible.

(b) The friction factor f remains constant over the entire interface; i.e., $f = f_i$.

Equation (17) can then be transformed into

$$p_a v_D/h = \bar{\sigma}_a (\dot{\bar{\epsilon}}_a + f\ \Sigma I_i/V) \tag{18}$$

and, with

$$\bar{\sigma} = C\dot{\bar{\epsilon}}^m ,$$

$$p_a = \frac{h}{v_D} C\dot{\bar{\epsilon}}_a{}^m (\dot{\bar{\epsilon}}_a + f\ \Sigma I_i/V) \quad . \tag{19}$$

Equation (19) illustrates the relationship between the forming pressure, the properties of the deforming material (flow stress, strain-rate dependency), and the friction at the interface. Heuer[6] derived Equation (19) by neglecting the interface friction and pointed out that by using the same equation the average strain rate, $\dot{\bar{\epsilon}}_a$, can be determined from a model test. Then the forming pressure, p_a, can be calculated for the real test as long as the C and m values of both real and model materials are known.

Approximate Similarity in Strain-Hardening Materials

The model and the real materials are both assumed to be strain dependent according to $\bar{\sigma}_M = K_M \bar{\epsilon}^{n_M}$ and $\bar{\sigma}_R = K_R \bar{\epsilon}^{n_R}$, respectively. Then, with $dV = A \cdot dh$ and $V_D = \frac{dh}{dt}$, Equation (13) gives

$$p_a \cdot A \cdot \frac{dh}{dt} \cdot dt = A \int_o^{\bar{\epsilon}} \bar{\sigma} d\bar{\epsilon} dh + \int_F f \bar{\sigma} v_F \cdot dF dt \quad . \tag{20}$$

With Equation (15c) and by defining the average strain, $\bar{\epsilon}_a$, and average flow stress, $\bar{\sigma}_a$, as $\int_o^{\bar{\epsilon}} \bar{\sigma} d\bar{\epsilon} = \bar{\sigma}_a \cdot \bar{\epsilon}_a$, Equation (20) gives

$$p_a A = A \bar{\sigma}_a \cdot \bar{\epsilon}_a + \frac{1}{v_D} \Sigma f_i \bar{\sigma}_i I_i \quad . \tag{21}$$

Again with $\bar{\sigma}_a \simeq \bar{\sigma}_i$, $f_i = f$ and with $\bar{\sigma}_a = K \bar{\epsilon}_a^{\,n}$

$$p_a = K \bar{\epsilon}_a^{\,n} \left(\bar{\epsilon}_a + f \frac{\Sigma I_i}{v_D A} \right) \quad . \tag{22}$$

Equation (22) corresponds essentially to Equation (19) and is to be used with strain-dependent materials. For n = o and f = o, Equation (22) gives

$$p_a = K \bar{\epsilon}_a^{\,n+1} \text{ or } \bar{\epsilon}_a = \left(\frac{p_a}{K} \right)^{\frac{1}{n+1}} \quad . \tag{22a}$$

Equation (22a) is exactly the same as the relation derived by Kashar[11] who assumed and proved experimentally that in extrusion $\bar{\epsilon}_a = a + b \ln R$, where,

R = extrusion ratio

a, b = constants dependent upon die geometry and flow conditions.

It should be noted that the above derivations are made by considering the deformation during a small time element, dt. Therefore, Equations (19) and (22) are both valid also in case of non-steady-state processes. In non-steady-state deformation the velocity field, and consequently the strain and the strain-rate distributions, vary continuously during deformation. Therefore, the concepts of average flow stress, $\bar{\sigma}_a$, average strain, $\bar{\epsilon}_a$, and average strain rate, $\dot{\bar{\epsilon}}_a$, are valid only for a stage of deformation during a small time interval, dt. In this case, the process must be studied in small steps; i.e., $\bar{\sigma}_a$, $\bar{\epsilon}_a$, $\dot{\bar{\epsilon}}_a$ must be determined at a given stage for a small time interval, dt. The same similarity conditions will apply between real and model tests at each corresponding stage of deformation.

Determination of Friction Energy in a Model Test

Equations (19) and (22) both give the average forming pressure in terms of the kinematics of the deformation zone as expressed by average strain, $\bar{\epsilon}_a$, and average strain rate, $\dot{\bar{\epsilon}}_a$, and in terms of friction conditions as expressed by f and ΣI_i in Equation (15c). It should be noted that the values of $\frac{\Sigma I_i}{V}$ and $\frac{\Sigma I_i}{v_D A}$ correspond to the well-known surface-to-volume ratio of deforming material and are solely dependent upon the kinematics of deformation.

In order to determine the friction energy in Equation (15c), values for I_i must be obtained and f must be estimated. This can be done by experimentally determining the velocities at the interface from the model test, e.g., by studying the grid-line distortions on the surface of a sample. The integrals $\int_F v_i dF$ of Equation (15c) can then be evaluated. Another way is to perform two model tests with two different model materials. In the strain-hardening case, for instance, from Equation (22):

$$p_{a1} = K_1 \bar{\epsilon}_a^{n_1} \left(\bar{\epsilon}_a + \frac{f \cdot \Sigma I_i}{v_D \cdot A} \right) \tag{23a}$$

$$p_{a2} = K_2 \bar{\epsilon}_a^{n_2} \left(\bar{\epsilon}_a + \frac{f \cdot \Sigma I_i}{v_D \cdot A} \right) . \tag{23b}$$

For similar friction conditions and similar flow, the expressions in the parentheses are the same for both tests. Therefore,

$$\frac{p_{a1}}{p_{a2}} = \frac{K_1}{K_2} (\bar{\epsilon}_a)^{n_1 - n_2} \tag{24a}$$

or

$$\bar{\epsilon}_a = \left(\frac{p_{a1}}{p_{a2}} \cdot \frac{K_2}{K_1} \right)^{\frac{1}{n_1 - n_2}} . \tag{24b}$$

The average strain, $\bar{\epsilon}_a$, is determined and from Equation (23a) or Equation (23b) the friction component, $\frac{f \cdot \Sigma I_i}{v_D \cdot A}$, can be calculated. Consequently, p_a for the real test can be estimated with Equation (22). The same procedure can be used with strain-rate-dependent model materials.

One strain-hardening-dependent material (subscript 2) and one strain-rate-dependent material (subscript 1) can also be used, for instance, plasticine and lead. Then,

$$p_{a1} = \frac{h}{v_D} \cdot C_1 \dot{\bar{\epsilon}}^{m_1} \left(\dot{\bar{\epsilon}} + \frac{f \cdot \Sigma I_i}{h \cdot A} \right) \quad . \tag{25a}$$

With $\dot{\bar{\epsilon}}_a = \bar{\epsilon}_a \cdot \frac{v_D}{h}$,

Equation (25a) transforms into

$$p_{a1} = C_1 \bar{\epsilon}^{m_1} \left(\frac{v_D}{h} \right)^{m_1} \left(\bar{\epsilon}_a + \frac{f \cdot \Sigma I_i}{v_D \cdot A} \right) \quad . \tag{25b}$$

With Equation (22) and similar friction conditions,

$$\bar{\epsilon} = \left[\frac{p_{a1}}{p_{a2}} \cdot \frac{K_1}{K_2} \left(\frac{h}{v_D} \right)^{m_1} \right]^{\frac{1}{m_1 - n_1}} \quad . \tag{26}$$

Using Equations (26) and (25b), the average strain, $\bar{\epsilon}$, and the friction component, $f\Sigma I_i$, can be determined and used for estimating p_a for the real test.

Application of Approximate Similarity in Prediction of Forming Pressures in Extrusion

In order to verify the approximate similarity experimentally, gray plasticine was chosen as model material to simulate cold forming of steel. Plasticine has already been used by other workers[1, 2, 7] to study metal flow and gray plasticine is readily available.

Properties of Plasticine

It is widely reported that plasticine is a strain-hardening material with small strain-rate dependency at room temperature, except at very low strain rates.[7] Figure 4 shows flow stress versus effective strain data for gray plasticine at two different ram speeds (0.2 in./min and 2.0 in./min). The difference between the two curves is within the range of experimental variation. These results are in agreement with Brill's studies on the flow behavior of plasticine[7], as seen in Figure 5. Actual samples (1 inch in diameter by 1 inch high) upset to 50 percent of original height are

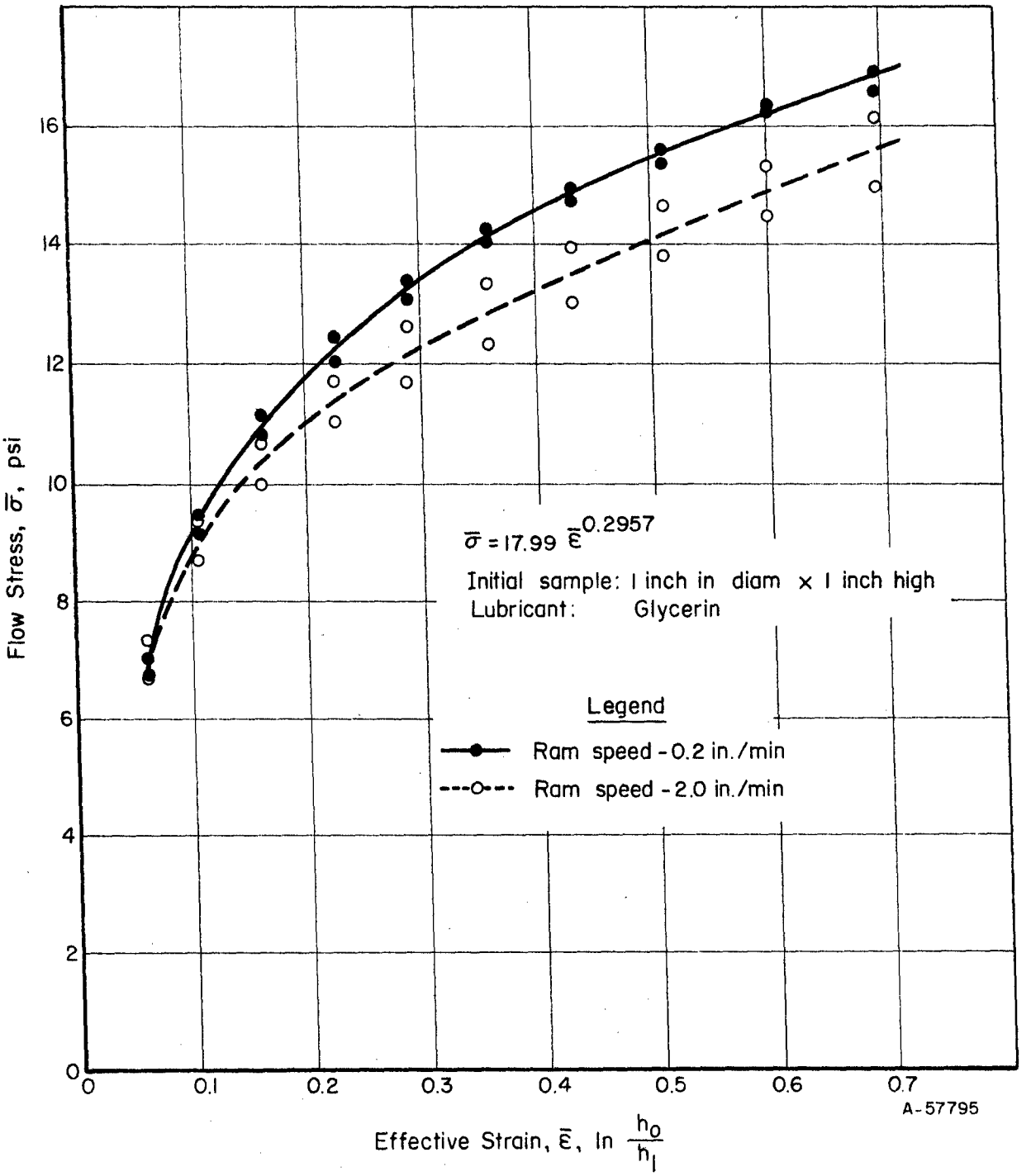

FIGURE 4. COMPRESSIVE FLOW STRESS VERSUS STRAIN FOR GRAY PLASTICINE USED IN BACKWARD EXTRUSION TESTS

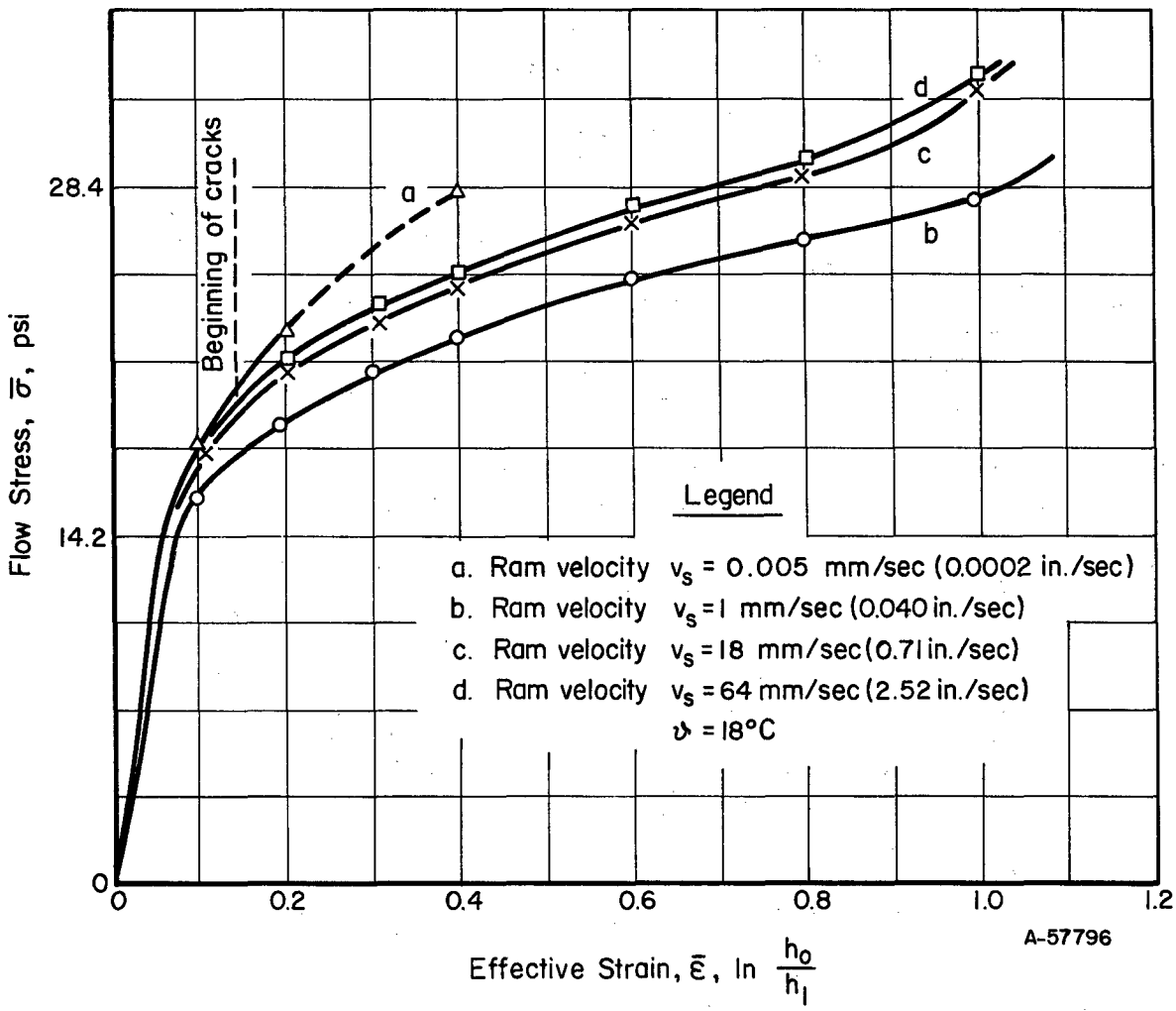

FIGURE 5. COMPRESSIVE FLOW STRESS VERSUS STRAIN FOR WHITE PLASTICINE AT DIFFERENT RAM VELOCITIES[7]

shown in Figure 6. The sample in the center of Figure 6 was upset to 35 percent, at which point it cracked. Glycerin was used as a lubricant and barrelling was essentially eliminated throughout the compression test except toward the final stage. An X-Y plotter connected to the testing machine recorded the load versus displacement during the compression tests. The instantaneous surface was calculated from the instantaneous height, h, and from the initial volume, $V = \frac{\pi D^2}{4} \cdot h_o$. A computer program with least-mean-square fit was used for fitting the stress-strain data to the exponential form $\bar{\sigma} = K\bar{\epsilon}^n$, and for determining the values of K and n.

The following observations are useful in working with plasticine:

(a) Plasticine has a low flow stress ($\simeq$ 15-30 psi) and can be used with relatively simple and inexpensive tooling.

(b) The flow stress versus strain data can be approximated in exponential form, $\bar{\sigma} = K\bar{\epsilon}^n$.

(c) At room temperature, plasticine is not strain-rate dependent except at very low strain rates where its workability decreases considerably. This is illustrated in Figure 6. The tests were stopped as soon as rupture occurred. The same observation was made by Brill[7] in upsetting white plasticine at 0.005 mm/sec ($\simeq$ 0.118 in./min) ram speed, as indicated in Figure 5.

(d) In the range of normal room temperatures, the effect of minor temperature changes upon plasticine is insignificant.

(e) The flow stress of plasticine varies significantly from batch to batch. Essentially a mixture of solid particles in oil, plasticine apparently dries when exposed to air for long periods of time (weeks or months). It is therefore essential to obtain the stress-strain data on the modeling material in the same day as the model experiments are carried out. Comparison of Figures 4 and 9, for example, show a difference in flow-stress values between two batches of gray plasticine of about 30 to 40 percent.

(f) Before use, the plasticine must be well kneaded, and forged or extruded in order to eliminate air pockets which might remain in the material.

The plasticine samples used in compression and extrusion experiments were first hand kneaded, extruded to 1-inch-diameter samples, and then cut to the desired length with a wire cutter.

Extrusion of Gray Plasticine

Existing tooling, built for backward cup and forward rod extrusion of steel, was used in these experiments. The main components of the tooling are illustrated in Figure 7. If new tooling was to be built, mild steel or epoxy would have been completely

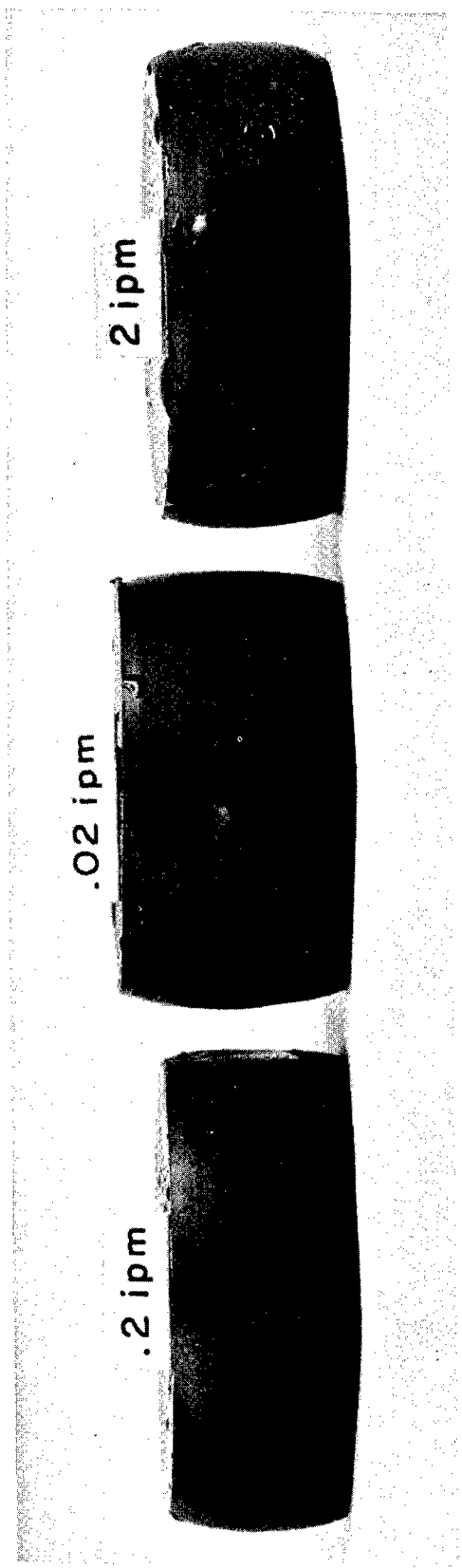

FIGURE 6. GRAY PLASTICINE SAMPLES COMPRESSED AT DIFFERENT RAM SPEEDS

Lubricant: Glycerin
Original Dimensions: 1-inch diameter by 1-inch height

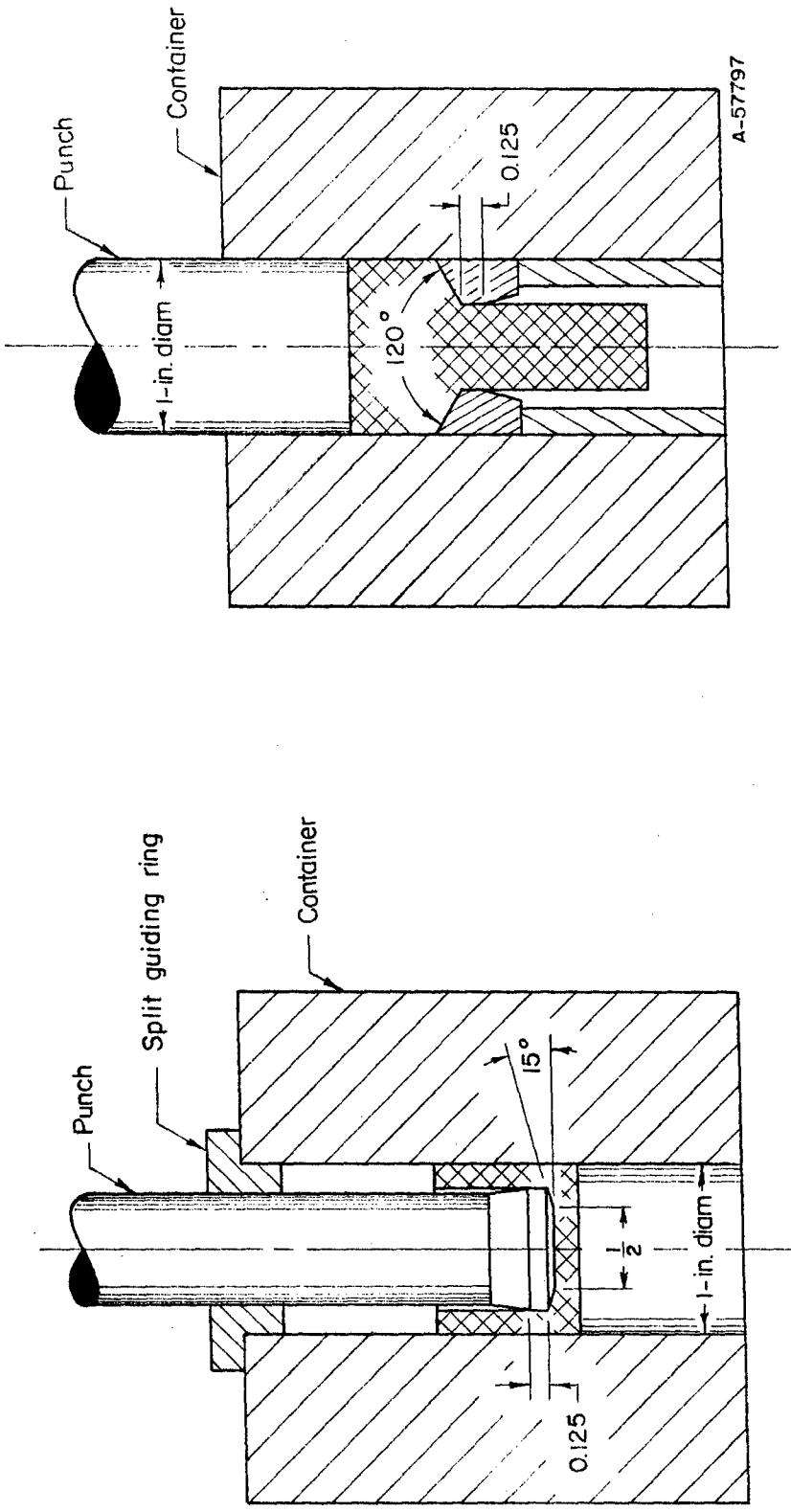

b. Forward Rod Extrusion

a. Backward Cup Extrusion

FIGURE 7. TOOLING USED IN EXTRUSION OF GRAY PLASTICINE

adequate for the model tool material. The extrusions were carried out with a testing machine at 0.2 in./min ram speed, and load versus displacement was recorded. Glycerin was used as lubricant in all tests.

Backward Cup Extrusion. The backward cup extrusion tooling is illustrated in Figure 7a. Two punch configurations were used: one with a 0.090-inch edge radius, the other with a 0.005-inch edge radius. All plasticine samples were 1 inch in diameter by 0.5 inch high. At the start of the extrusion, the punch was guided in the die by means of a split ring. When 0.050-inch displacement was reached, the ram was stopped and the split guiding rings were removed while maintaining the load. The self-centering punch was then moved farther until the total travel of 0.400 inch was completed. The punch load versus displacement curves for different extrusion ratios are given in Figure 8.

Flow stress-strain data for the gray plasticine used in these series of extrusions were obtained from compression tests using 1-inch-diameter by 1-inch-high plasticine samples (Figure 4).

Forward Rod Extrusion. For these experiments, another batch of gray plasticine was used. The stress versus strain data are given in Figure 9. All extrusion samples were 1 inch in diameter by 1.5 inch long and were extruded to 0.5-inch butt length through three 120-degree included-angle dies to produce 20, 50, and 70 percent reduction. The forward extrusion tooling is illustrated in Figure 7b. The punch load versus displacement curves are given in Figure 10.

A typical load-displacement curve for steel extrusion is given in Figure 11. Comparison with Figure 10 shows that the load curves for plasticine at 70 and 50 percent reduction do not have quite the same shape as that for steel. The "peak" or breakthrough loads are not as distinct for the plasticine extrusions. This can be expected especially for larger reductions where the contribution of friction forces to the overall load is proportionately smaller in extrusion of plasticine than in extrusion of steel. For smaller reductions, such as 20 percent, the wall friction in the extrusion container is proportionately higher. This is probably due to the dependency of the coefficient of friction upon the normal stress at the interface. This variation was reported by Brill[7] who measured the coefficient of friction, μ, between white plasticine and steel at different normal stresses with machine oil as the lubricant. Brill observed that the coefficient of friction decreased about 30 percent (0.03 to 0.023) with a threefold increase in normal stress (6 psi to 18 psi) at an interface velocity of 0.060 in./sec.

Prediction of Punch Pressures in Backward Extrusion of Steel

In backward extrusion, the load remains essentially constant, as seen in Figures 8 and 11, as do the punch and the extrusion pressures. The slight increase in load observed with plasticine is due to friction between the tools and the extruded plasticine cup. As shown in Figure 8, the change in punch radius altered the punch load 2 pounds, which was not considered significant at the extrusion ratios investigated. Therefore, the average value at 0.2-inch displacement was used as constant punch load for all

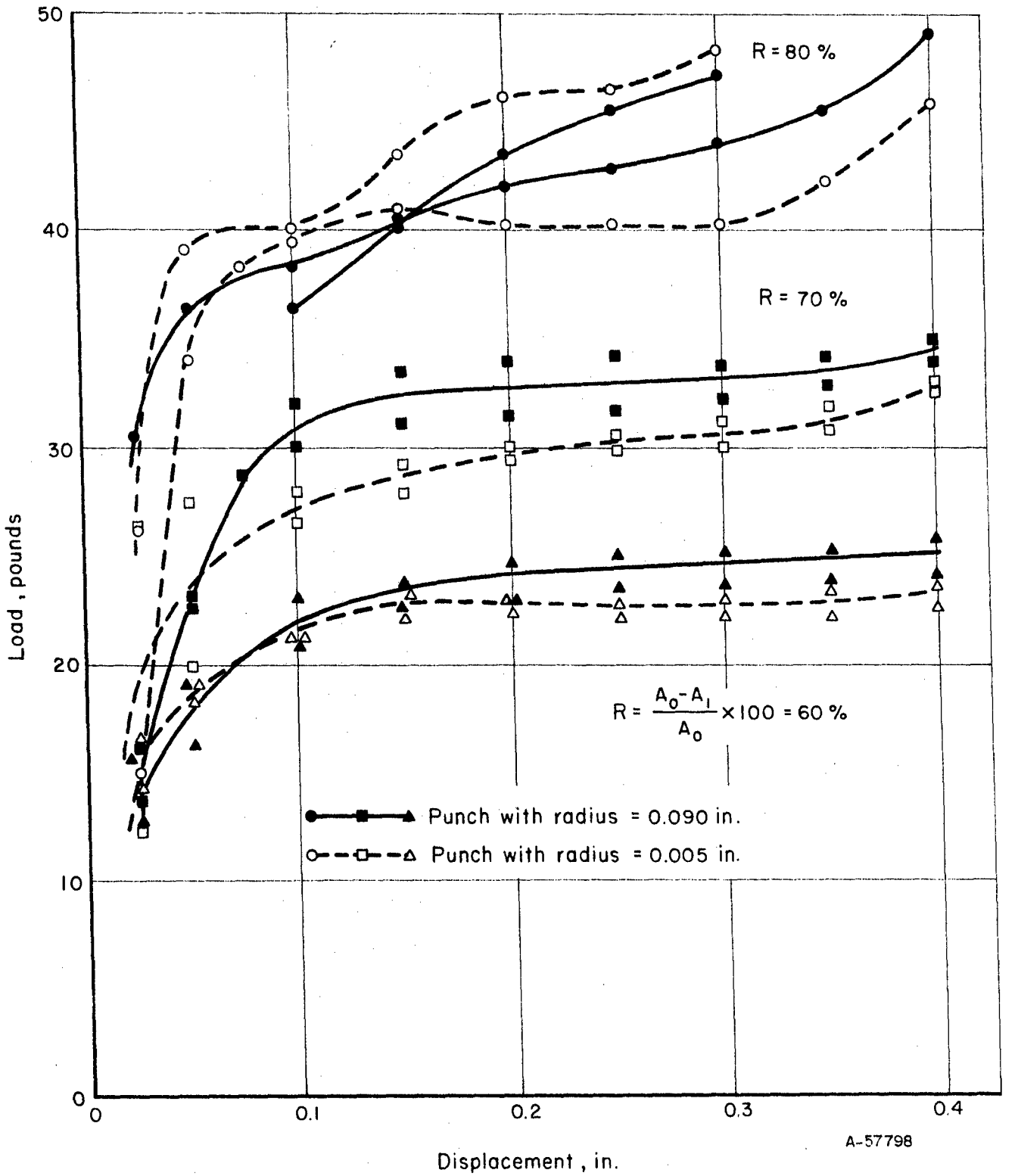

FIGURE 8. LOAD VERSUS DISPLACEMENT IN BACKWARD EXTRUSION OF GRAY PLASTICINE AT DIFFERENT REDUCTIONS

Samples: 1 inch in diameter by 0.5 inch high.
Lubricant: Glycerin
Ram Speed: 0.2 in./min.
Flow stress versus strain curve for Plasticine given in Figure 4.

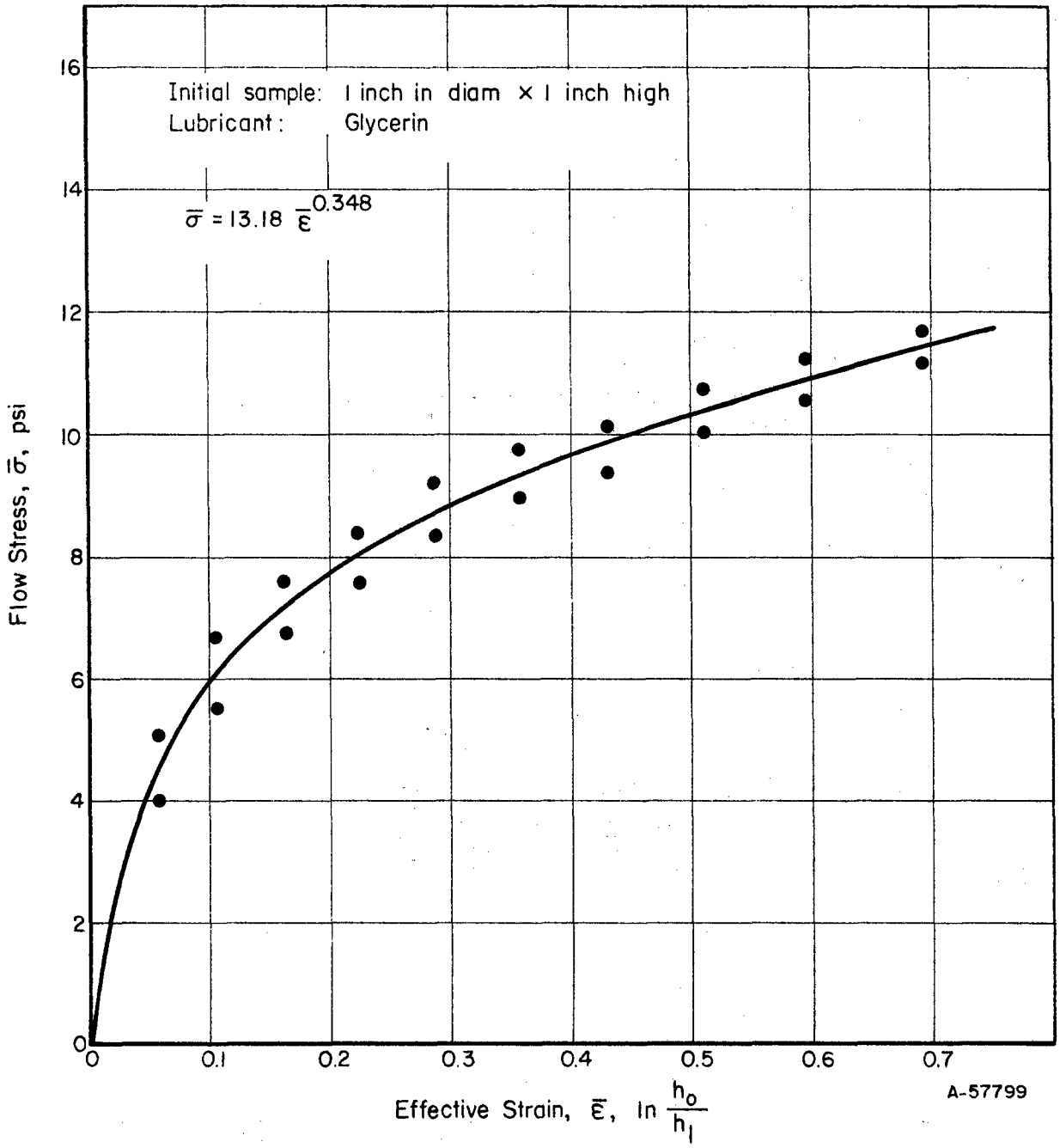

FIGURE 9. COMPRESSIVE FLOW STRESS VERSUS STRAIN FOR GRAY PLASTICINE USED IN FORWARD EXTRUSION TESTS

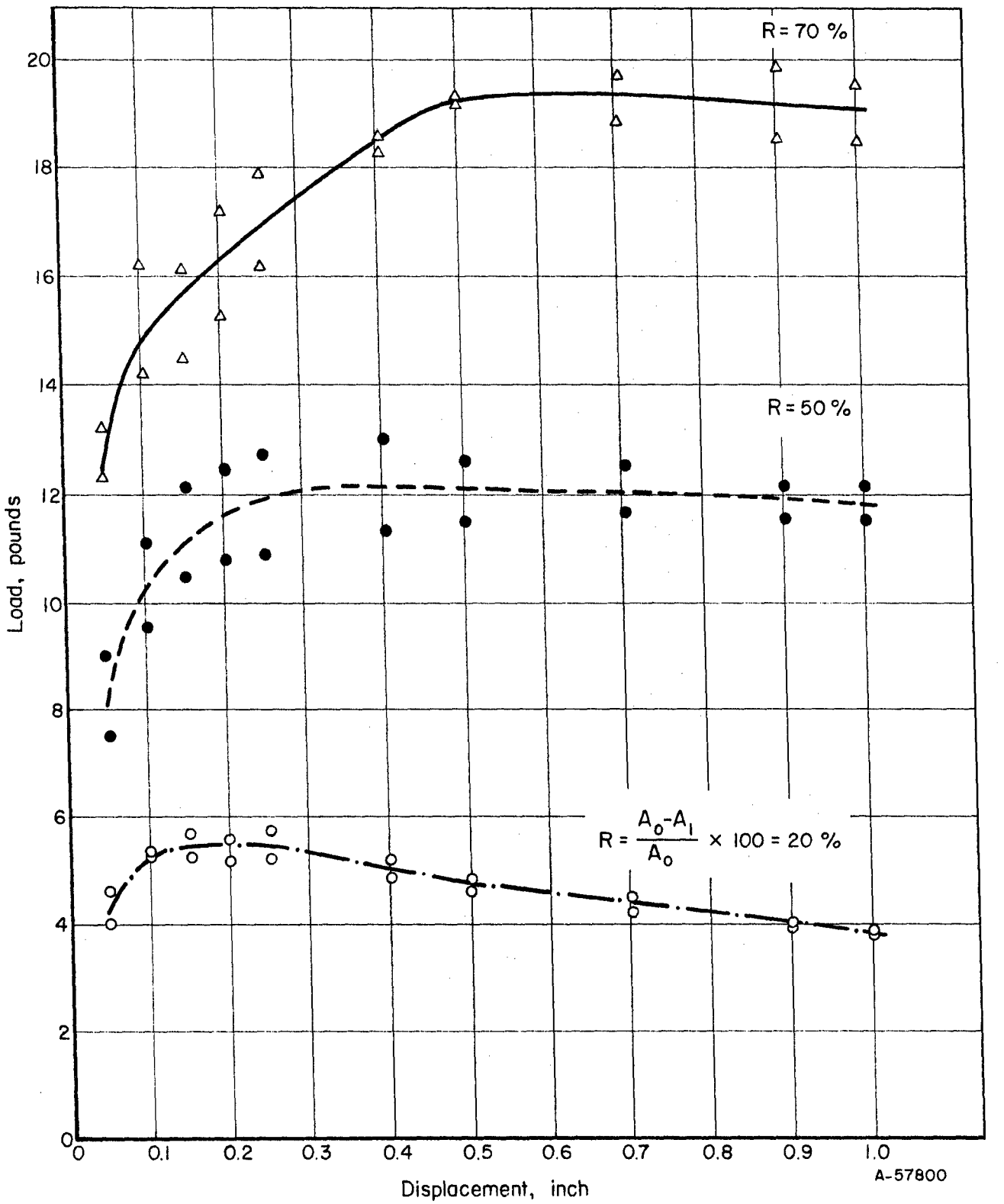

FIGURE 10. LOAD VERSUS DISPLACEMENT IN FORWARD EXTRUSION OF GRAY PLASTICINE AT DIFFERENT REDUCTIONS

Samples: 1 inch in diameter by 1.5 inch long
Lubricant: Glycerin
Ram Speed: 0.2 in./min.

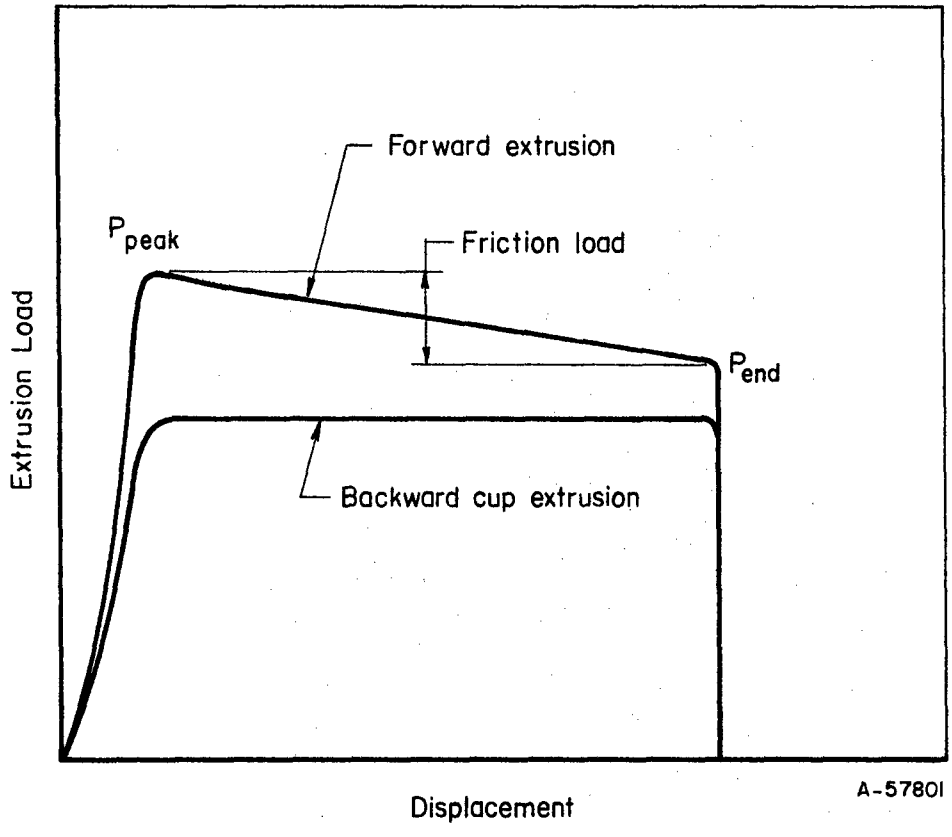

FIGURE 11. TYPICAL SHAPES OF LOAD-DISPLACEMENT CURVES IN COLD EXTRUSION OF STEEL

backward extrusions of plasticine, and average values of two punches were used for steels. The same tooling was used in extrusion of both materials. The extrusion pressure measured in extruding plasticine was used for predicting the extrusion pressures for steels.

The average value of the extrusion pressure is

$$p_a = \frac{p \cdot 4}{\pi D^2} \tag{27}$$

In all extrusions gray plasticine was well lubricated with glycerin, while standard zinc phosphate-stearate lubrication was used with steel extrusions. Assuming that lubrication was adequate and the friction force was negligible compared with the overall forming force, Equation (22) reduces to

$$p_a = K\bar{\epsilon}_a^{\,n+1} \quad . \tag{28}$$

Using the known values of Figure 4 in Equation (28), the average strain, $\bar{\epsilon}_a$, is determined from the plasticine tests:

$$\bar{\epsilon}_a = \left(\frac{p_a}{17.99}\right)^{\frac{1}{1.2957}} \quad . \tag{29}$$

The average extrusion pressure for a given steel is then found by reusing Equation (28). For 1005 steel, for instance, tensile data gave K = 86,000 psi and n = 0.250. Thus, for 1005,

$$p_a = 86,000(\bar{\epsilon}_a)^{1.250} \quad .$$

The punch pressure is then obtained from the extrusion ratio. For instance, for R = 80 percent, punch pressure = $\frac{p_a}{0.80}$.

The predicted pressures for some steels are given in Table 1 with actual measured punch pressures. Extrusion pressures calculated by using Equations (28) and (29) were usually higher than those measured in experiments on steels by about 1 to 20 percent. That agreement is considered within useful engineering accuracy.

Prediction of Pressures in Forward Extrusion of Steel

A typical load versus displacement curve for forward extrusion of steel is shown in Figure 11. The peak load, P_p, depends upon the initial length of the billet and upon the upsetting and friction conditions in the container. The actual extrusion load due to deformation is better represented by the end load, P_e, of Figure 10. The end load at 1.0-inch displacement during the extrusion of gray plasticine was used to predict the end loads for various steel extrusions.

TABLE 1. PREDICTION OF PUNCH PRESSURES IN BACKWARD CUP EXTRUSION FROM MODEL TEST

Model Material: Gray Plasticine With $\bar{\sigma} = 17.99(\bar{\epsilon})^{0.2957}$

Material	K	n	Average Punch Pressures at Reductions Indicated[a], psi					
			R = 80 Percent		R = 70 Percent		R = 60 Percent	
			Predicted	Measured	Predicted	Measured	Predicted	Measured
Plasticine	17.99	0.2957	--	68.2 or $\bar{\epsilon}_a = 2.35$	--	59.5 or $\bar{\epsilon}_a = 1.915$	--	49.8 or $\bar{\epsilon}_a = 1.481$
1005	86,000	0.250	312,000	268,000	276,000	245,400	231,500	228,000
8620	120,000	0.173	399,000	Not available	354,000	341,000	318,000	309,000
10B18	115,000	0.212	394,000	Not available	360,000	312,000	308,000	290,000
1018	117,000	0.224	415,000	Not available	373,000	305,000	315,000	293,000
12L14	115,000	0.250	417,000	Not available	370,000	308,000	313,000	282,000

(a) Reduction, $R, = \frac{A_o - A_1}{A_o} \times 100.$

By neglecting the friction on the die surfaces, with Equations (27) and (28) and using the K and n values of plasticine (Figure 9),

$$\bar{\epsilon}_a = \left(\frac{p_a}{13.18}\right)^{\frac{1}{1.348}} \quad . \tag{30}$$

The end pressures are calculated for various steels with Equations (28) and (30). The predicted and measured pressures are given in Table 2. The agreement is reasonably good, within 10 percent, except in the case of 20 percent reduction, where the predicted values are lower. This might result from the shape of the load displacement curve for R = 20 percent, as seen in Figure 10. The friction component of total extrusion load appears to be significant in extruding plasticine to a 20 percent reduction. Another reason for disagreement between predicted and measured pressures might be "dead-metal" zone formation in extrusion of steel to a 20 percent reduction with a 120-degree die angle. In this case, a natural shearing angle forms and the material shears over itself instead of sliding along the die surface.

CONCLUSIONS AND FUTURE WORK

Model materials such as sodium and plasticine can be used for predicting loads in forming operations. Pressures predicted from modeling experiments are well within the range of engineering accuracy for the cold forming of several steels.

The analysis of interface friction in forming has been presented. In the prediction of extrusion loads, friction was neglected because only well-lubricated cold forming of steel was simulated. The analysis and the experimental verification must be extended to forming operations where friction forces are a large proportion of the overall forming load and cannot be neglected as in hot forging.

Backward and forward extrusion simulated in the present study are essentially steady-state deformation processes. The velocity and strain fields, and consequently the average strain, $\bar{\epsilon}_a$, do not vary during the process, except when the bottom thickness of can or butt length of billet becomes very small. In non-steady-state processes, such as most forging operations, the metal flow, the velocity field, and the average strain, $\bar{\epsilon}_a$, and strain rate, $\dot{\bar{\epsilon}}_a$, vary continuously with time. A process of this sort must be investigated in small steps. At every deformation step a new $\bar{\epsilon}_a$ or $\dot{\bar{\epsilon}}_a$ must be used for predicting the load-displacement curve for the real test.

The work on model studies will be continued during the present program. The interface friction and the modeling of non-steady-state processes will be investigated in greater depth.

TABLE 2. PREDICTION OF PUNCH PRESSURES IN FORWARD ROD EXTRUSION FROM MODEL TEST

Model Material: Gray Plasticine With $\overline{\sigma} = 13.18\ (\overline{\epsilon})^{0.348}$

Material	K	n	Average Punch Pressures (End Load) at Reductions Indicated[a], psi					
			R = 70 Percent		R = 50 Percent		R = 20 Percent	
			Predicted	Measured	Predicted	Measured	Predicted	Measured
Gray Plasticine	13.18	0.348	--	24.3 or $\overline{\epsilon}_a = 1.575$	--	15.0 or $\overline{\epsilon}_a = 1.1014$	--	4.97 or $\overline{\epsilon}_a = 0.4875$
1005	86,000	0.250	151,000	157,000	97,000	96,000	35,000	49,000
1010	100,000	0.305	181,000	164,000	113,000	108,000	39,200	52,000
1010	94,000	0.300	169,500	146,300	106,700	101,000	37,000	48,000
1018	117,000	0.224	204,000	Not available	132,000	145,700	48,500	68,000
8620	120,000	0.173	204,500	Not available	134,500	145,000	51,400	69,000

(a) Reduction, $R, = \frac{A_o - A_1}{A_o} \times 100.$

REFERENCES

(1) Green, A. P., "The Use of Plasticine Models to Simulate the Plastic Flow of Metals", Phil. Mag., 42, 365-373 (April, 1951).

(2) Cook, P. M., "Use of Plasticine Models in Forging Research", Metal Treatment and Drop Forging, 541-598 (November, 1953).

(3) Holmquist, J. L., "Investigation of the Piercing Process by Means of Model Wax Billets", Iron & Steel Engineer, 25-40 (December, 1952).

(4) Chang, K. T., and Brittain, T. M., "An Investigation of Analog Materials for the Study of Deformations in Metal Processing Simulations", ASME Paper 67-WA Prod-9.

(5) Thomsen, E. G., Yang, C. T., and Kobayashi, S., Mechanics of Plastic Deformation in Metal Processing, The Macmillan Company, New York (1965).

(6) Heuer, P. J., "Modellverfahren für die Umformtechnik, Fliessvorgänge, Werkstoffkonstante, Umformbeiwert" (Modeling Methods for Forming Technology, Flow, Material Constant, Forming Factor), VDI Forschungsheft, 493 (1962)

(7) Brill, K., "Modellwerkstoffe für die Massivumformung von Metallen", (Model Materials for Forging of Metals), Dissertation, Hannover (1963).

(8) Hertel, Heinrich, "Modelltechnische Untersuchung der Fliessvorgänge beim Strang-und Gesenkpressen" (Simulated Investigation of Material Flow in Extrusion and Forging), Automobil-Industrie, 11, 3-12 (August 25, 1966).

(9) Pawelski, O., "Beitrag zur Ahnlichkeitstheorie der Umformtechnik" (Contribution to Theory of Similitude in Forming Technology), Archiv f. Eisenhüttenwesen, 35, 1-10 (1964).

(10) Kobayashi, S., "Dynamic Similitude in Materials Processing", Unpublished review on model tests in forming (1966).

(11) Kashar, L. J., "Prediction of Extrusion Pressures in Cold Forging of Steel", Trans. Met. Soc. of AIME, 239, 1461-1468 (1967).

LIST OF SYMBOLS

x = length

P = force, load

t = time

λ = scale factor of length

κ = scale factor of force

T = scale factor of time

$\bar{\sigma}$ = true flow stress of a deforming material

G = shear modulus

E = Young's modulus

A_o = original billet cross-sectional area

A_1 = cross-sectional area of extruded rod in forward extrusion, cross-sectional area of extruded can in backward extrusion

ρ = specific gravity

μ = coefficient of friction

$\bar{\epsilon}$ = effective strain

$\bar{\epsilon}_a$ = average effective strain in the deformation zone

$\dot{\bar{\epsilon}}$ = effective strain rate

$\dot{\bar{\epsilon}}_a$ = average effective strain rate in the deformation zone

θ = temperature

w = width of flash land

t = thickness of flash

p_a = average forming pressure
= average punch pressure in forward rod extrusion
= extrusion pressure in backward cup extrusion